INTERNATIONAL JOURNAL FOR NUMERICAL METHODS IN FLUIDS
Int. J. Numer. Meth. Fluids **26**: 837–850 (1998)

NUMERICAL MODELLING OF THERMAL RADIATION ABSORPTION DURING THE DISPERSION OF DENSE GAS CLOUDS IN THE ATMOSPHERE

A.I. SAYMA[a,*] AND P.L. BETTS[b]

[a] *Centre of Vibration Engineering, Department of Mechanical Engineering, Imperial College, London SW7 2BX, UK*
[b] *Department of Mechanical Engineering, UMIST, PO Box 88, Manchester, M60 1QD, UK*

SUMMARY

A numerical model is presented for the prediction of thermal radiation absorption in dense gas clouds during accidental release in the atmosphere. The model is based on the discrete transfer method (DT method) that was originally developed for modelling radiation in combustion chambers. The radiation model assumes a number of representative rays of predetermined orientation fired from each of the domain boundaries. Each ray is traced through the domain elements until reaching another boundary where it is terminated. Radiation sources are calculated for each element by performing an energy balance across each element for each ray passing through it. The energy sources recovered are fed into the finite element flow solver for every time step in the energy equation. The model proved accurate, and memory and computer time efficient. It showed that accounting for radiation effects lead to improved predictions. It also showed that in certain scenarios, radiation effects could be predominant. © 1998 John Wiley & Sons, Ltd.

KEY WORDS: dense gas dispersion; radiation absorption; discrete transfer method

1. INTRODUCTION

Many toxic or flammable gases are stored and transported at high pressure or low temperature, or both. If during the course of manufacture, transport or storage of these gases, an accidental release into the atmosphere occurs, the consequences could be fatal. By virtue of their molecular weight or temperature at release to the atmosphere, some gases could be denser than air. This results in a dense gas cloud which rolls near the ground for some time before dispersing, which increases the risks of suffocation, fires or explosions. The problem of estimating the consequences of dense gas releases in the atmosphere is of prime importance in the assessment of the safety of industrial installations or transport systems. The task of performing such an assessment has been introduced as a regulatory requirement in many countries. The assessment procedures depend mainly on experience from previous accidents, experimental tests conducted in laboratory or field tests and mathematical models.

The finite element code, FEMSET, has been developed by Betts and Haroutunian [1] to simulate the dispersion process of a dense gas cloud following an accidental release. The model is based on the Reynolds-averaged mean flow equations of mass, momentum, enthalpy, and

* Correspondence to: Centre of Vibration Engineering, Department of Mechanical Engineering, Imperial College, London SW7 2BX, UK.

CCC 0271–2091/98/070837–14$17.50

Received November 1996
Revised June 1997

species concentration. The eddy viscosity is modelled through extension of the standard two-equation $k-\epsilon$ model [2] to account for the anisotropy in turbulence resulting from buoyancy. The Galerkin finite element method is used to discretize the system of equations in space with trilinear isoparametric brick elements for all variables except the piecewise constant for pressure. The explicit forward Euler method is used to advance the resulting system of equations in time. The balancing tensor diffusion (BTD) [3] is used to counter the negative diffusivity resulting from the truncation error resulting from the explicit Euler method, by adding an equal amount of diffusion. The model was extended to accommodate irregular topography problems while retaining computational accuracy and economy using an improved near-ground treatment [4,5]. In this treatment, a one element-thick layer of special elements is used to bridge the gap between the main domain of all equations, including k and ϵ and the solid boundary. In this layer, a special shape function derived from the logarithmic boundary layer profiles is used to resolve the sharply varying quantities in the near wall region.

The code was tested over a wide range of 2D flows and was found to be a robust general purpose two-equation flow solver. Dense gas dispersion simulations, conducted to simulate field and laboratory tests [4,6,7], showed that the code is a useful tool in understanding and predicting dense gas dispersion scenarios. However, certain areas have been identified for further improvement and development.

Numerical simulation of the Burro-8 dense gas dispersion field trial [8] showed that local collapse of turbulence occurred in regions around the dense gas source and downstream of the source. Although the collapse of turbulence could occur naturally due to the strong stratification resulting from the severe temperature gradients in the dense gas cloud, overprediction of the collapse was apparent from the prediction of a wider and lower cloud compared with the experiment. This overprediction was referred partly to the inability of the high Reynolds number turbulence model to predict the laminarisation process and partly to the underprediction of the heat input to the cloud from the surroundings. In the present model, heat transfers to the cloud through two mechanisms. The first is the ground heat applied through the boundary conditions. The second is the turbulent mixing of the cloud with the surrounding air. Two potentially important sources of heat were not modelled. These are the thermal radiation absorption and the heat released during the condensation of water vapour. Since no previous attempt was made to study the effects of radiation absorption on the heat transfer process, the present study was undertaken to select and implement a suitable radiation model and to study this important phenomenon.

There are several numerical methods in the literature for predicting radiation absorption in participating media. For example, the zone method [11], the Monte Carlo method [12] and flux models [13]. In the zone method, the domain and the boundaries are divided into zones, which do not necessarily need to coincide with the fluids mesh. Direct exchange areas are defined for all zones that are used to compute the view factor between each pair of zones. The radiative exchange between each pair of zones is then calculated using the integrated form of the equation of transfer. This procedure results in a system of $n_z^2 \times n_z^2$ simultaneous algebraic equations, where n_z is the number of zones that need to be solved to produce the required energy transfers.

The Monte Carlo technique is a method of statistical sampling of events, to determine the average behaviour of a system. In radiative transfer, the method depends on following a finite number of randomly generated energy bundles through their transport histories within the system. The radiative behaviour of the system is then determined from the average behaviour of a number of these bundles. The technique is well-known for its large computational requirements.

The basic idea in flux models is to separate directional dependence from the spatial dependence of the intensity in the equation of radiative transfer. Hence, the integro-differential equation reduces to a system of differential equations. There is a wide range of flux models which treat the problem in different mathematical approaches, but they all fall within two categories: the continuous type and the discontinuous type. In the continuous type, the flux around a point is assumed to follow continuous variation while in the discontinuous type, the flux may take discrete values. In all the flux methods, the equation of transfer is expanded using a series expansion and this results in a set of first-order differential equations. In principle, the number of equations equals the number of terms retained in the series expansions or the number of fluxes considered. For some flux methods, this can be easily reduced to a lower number of higher-order differential equations. The larger the number of equations, the larger the number of coefficients to be stored per computational node. The most important drawback of flux models is the limited range of application of a certain model. This arises from the fact that certain series expansions will fit certain situations better because of the nature of the solution. Hence, methods that work in certain co-ordinate systems may not necessarily perform equally well in other systems.

Initial evaluation of above methods, showed that they are impractical for large scale 3D dense gas dispersion problems due to the prohibitive computational requirements involved. Attention was directed to an accurate and economical method developed by Lockwood and Shah [9] for radiation modelling in combustion chambers. This method is called the discrete transfer method (DT method). The method can be viewed as a blend of the zone method and flux models. It depends on firing a predetermined amount of arrays, in predetermined directions, from the nodes on the solution domain boundaries. The equation of transfer is solved recursively along these rays to solve for the unknown quantities.

In the present study, the DT method was adapted for dense gas dispersion problems, programmed and tested using standard analytical solutions. The tests demonstrated the accuracy and computational economy of the method. The dense gas dispersion model, with radiation modelling included, was then used to simulate the Burro-8 field trial over flat grounds, which was simulated earlier without modelling radiation. The predictions showed considerable improvements in the predictions when compared with the experimental results. Hypothetical tests for other scenarios showed that radiation absorption could transform a dense gas cloud to a buoyant plume quickly.

2. THE RADIATION MODEL

The fundamental equation for transfer of thermal radiation may be expressed as

$$\frac{\mathrm{d}I_v}{\mathrm{d}s} = k_v(-I_v + B_v(T)), \tag{1}$$

where effects of scattering have been neglected; scattering effects will be important in media containing particulate materials. In this equation, $I_v(s, \hat{\Omega}, t)$ is the intensity of a beam of monochromatic radiation travelling in the direction $\hat{\Omega}$, along path s and is a function of time t. Moreover, k_v is the monochromatic absorption coefficient and $B_v(T)$ is the Planck function which gives the monochromatic emissive power from the equation

$$B_v(T) = \frac{2hv^3}{c^2(e^{(hv/\kappa T)} - 1)}, \tag{2}$$

Table I. Wall fluxes for one-dimensional geometry

k_aL	$q_w/\sigma T_g^4$	
	Analytical	DT
0.1	0.1663	0.1749
0.5	0.5531	0.5612
1.0	0.7758	0.7875
1.5	0.8810	0.8899
2.0	0.9339	0.9430
2.5	0.9614	0.9705
3.0	0.9761	0.9850

where T is the local absolute temperature, c is the speed of light, $h = 6.6256 \times 10^{-34}$ J s is Planck's constant, $\kappa = 1.3805 \times 10^{-23}$ J (molecule K)$^{-1}$ is the Boltzman constant and v is the frequency.

Equation (1) can only be solved analytically for simple geometries with some simplifying assumptions. Some of these solutions have been presented by Chandrasekhar [10]. For practical engineering applications, it has to be solved numerically. In the present study, the DT method of Lockwood and Shah [9] has been adapted to suit the situations encountered in dense gas dispersion problems.

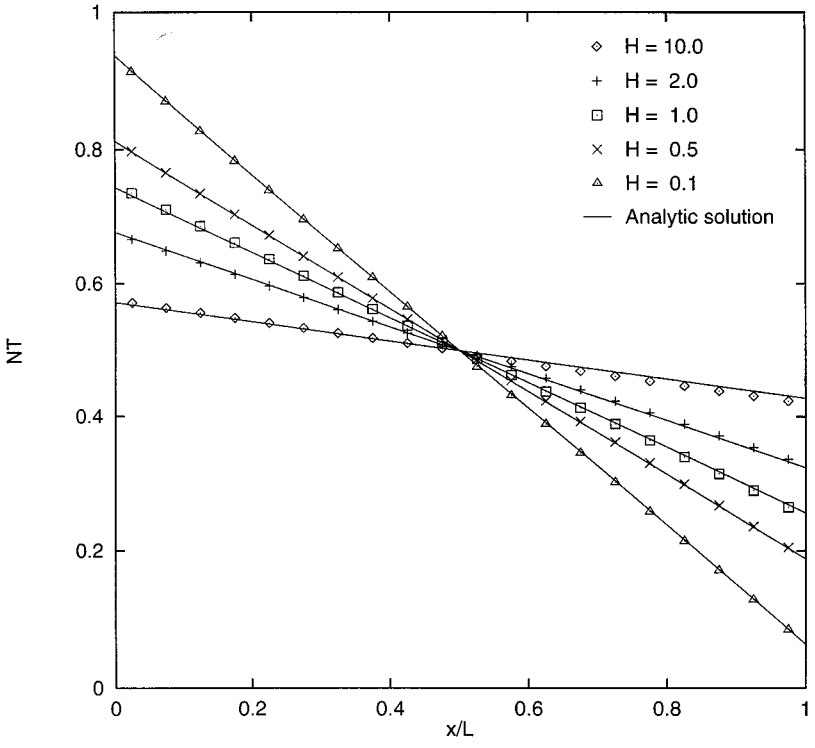

Figure 1. Predicted non-dimensional temperature distribution between two infinite black plates of temperatures T_1 and T_2 and distance L compared with the analytical solution, $NT = (T^4 - T_1^4)/(T_2^4 - T_1^4)$, $H = k_bL$.

Table II. Percentage error of energy sources calculated using the DT method compared with the analytical solution

Number of rays	10	20	30	40	50	100
% Error	11.40	3.01	1.22	0.61	0.37	0.07

Since absorption in gases occurs in narrow bands of the radiation spectrum and is essentially zero outside these bands, non-grey behaviour must be considered. For a gas with several absorption bands, the intensity and absorptivity are assumed constant for each band, where their values are taken as the average at that band. Equation (1) is then integrated over each band to give

$$\frac{\mathrm{d}I_b}{\mathrm{d}s} = k_b(-I_b + B_b(T)), \tag{3}$$

where I_b and k_b are the average intensity and absorptivity across the band, respectively, and $B_b(T)$ is the integrated emissive power across the same band.

In the DT method, Equation (3) is solved for each band to recover the energy sources in each element of the domain in the given band as follows.

For a collimated (i.e. non-diverging) ray, Equation (3) can be integrated analytically along any segment s of the ray, from position n to position $n+1$, where the absorption coefficient

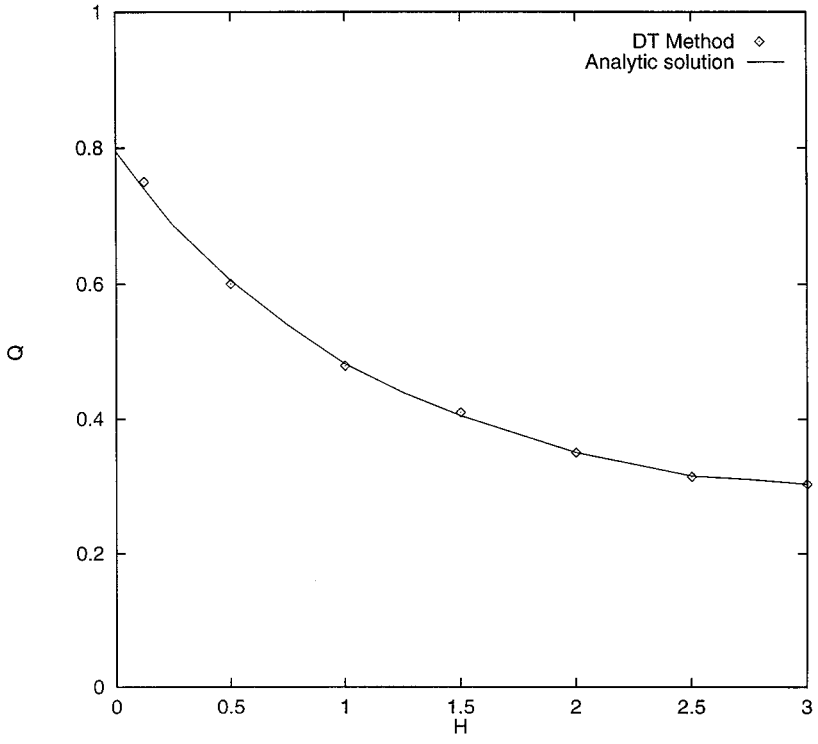

Figure 2. Predicted non-dimensional heat source distribution between two infinite plates, one is black and the other is grey of emissivity 0.8, compared with the analytical solution, $Q = q/\sigma(T_1^4 - T_2^4)$, q is the heat source per unit volume.

and temperature are assumed to be constant around that segment to produce the following recurrence relation

$$I_b^{n+1} = B_b(T)(1 - \mathrm{e}^{-k_b s}) + I_b^n \mathrm{e}^{-k_b s}. \tag{4}$$

The numerical procedure emerges from Equation (4) and can be described by the following steps.

- The domain under consideration is divided to n_e elements or 'cells', with all properties considered constant over each element. This requires averaging properties from their nodal values within the finite element mesh over each element.
- A number of rays of predetermined orientation is fired from the centroid of each face of the elements lying on the boundaries of the domain. The orientation of the rays can be arbitrary. However, in the present model, it is determined by dividing the half solid angle around the face's centroid into segments of equal angular divisions in both polar and azimuth directions. The rays then emerge from the central position of each segment. Each array is assumed to be collimated and to represent all the rays emerging from the segment. For curved boundary faces, the solid angle is that around the tangent surface to the face at it's centroid.
- For a known intensity of each ray at its origin (say I_0, which is determined from the boundary conditions), Equation (4) can be solved for intensity along the ray within each of the elements that it passes through, until it reaches another boundary where it is terminated. Diffusely reflected rays are accounted for through the boundary conditions relationship below.
- The source/sink in the energy equation for each element due to radiation absorption is calculated by performing an energy balance on each element using all the rays passing through it. That is

$$S_e = \sum_{j=1}^{nb} \sum_{i=1}^{m} (I_b^{n+1} - I_b^n)\, \mathrm{d}\Omega \underline{\Omega}\ \ \underline{\mathrm{d}A}\ , \tag{5}$$

  where m indicates the number of rays passing through the element under consideration, nb is the number of bands, S_e is the energy source/sink in element e, $\mathrm{d}\Omega$ is the portion of the solid angle from which the ray emerged and $\underline{\Omega}$ is a unit vector in the direction of the ray. The elemental area $\underline{\mathrm{d}A}$ is a vector of magnitude equal to the area of the surface of the element from which the ray is fired, and a direction normal to the surface at the centroid of that surface.
- Boundary conditions are determined according to the type of wall where the rays originate. If the wall is black, then the intensity I_0 is calculated from

$$I_0 = \frac{\sigma T_w^4}{\pi}, \tag{6}$$

  where T_w is the wall temperature and σ is the Stefan–Boltzman constant. If the wall is grey with emissivity ϵ_h then

$$I_0 = (1 - \epsilon_h)\frac{q^-}{\pi} + \epsilon_h \frac{\sigma T_w^4}{\pi}, \tag{7}$$

  where q^- is the incoming radiation flux to the wall calculated by computing the total incoming flux to the wall. This can be achieved by tracing the rays fired from the face until they reach another wall. Then the equation of transfer is solved along the ray from its

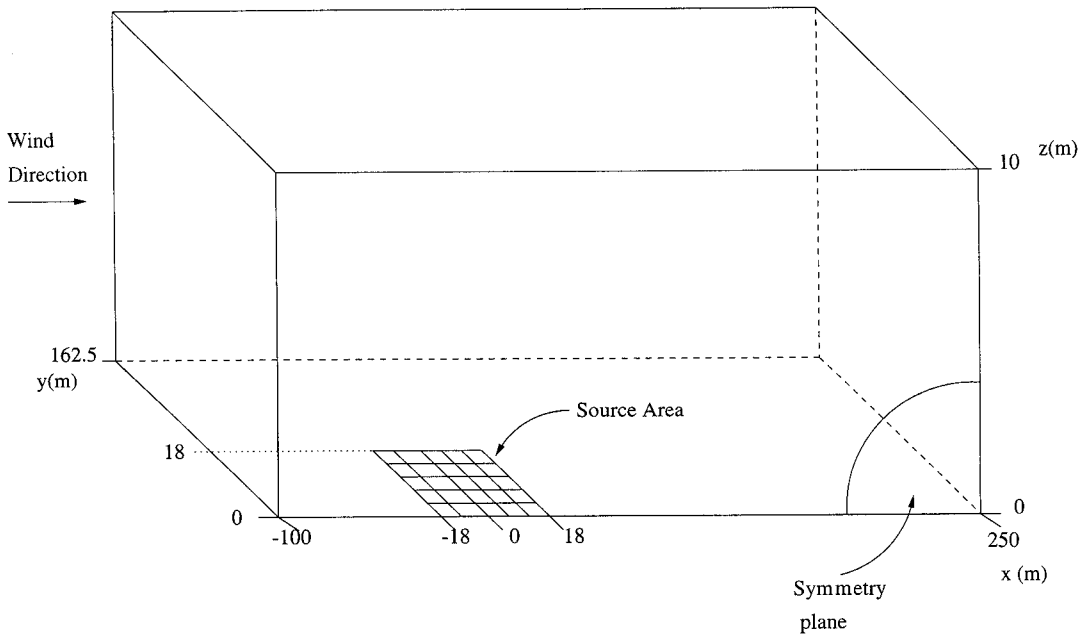

Figure 3. Schematic diagram of the solution domain

destination down to its origin. Consequently, if more than one wall is grey, the solution should evolve iteratively.

For problems of dense gas dispersion in the atmosphere, the solution domain for the radiative transfer can be imagined as that of a domain lying between two surfaces, the ground and a plane at the top of the solution domain, which represents the incoming solar radiation. Thus, the top of the domain can be considered as a black body of emissive power equal to the solar irradiation. The vertical sides are treated as planes of symmetry. For these planes, rays are reflected as if the plane was a mirror. So, the only grey boundary is the ground, and consequently, no iteration is required to determine the boundary conditions. The numerical algorithm starts by tracing the rays emerging from the ground until they reach the top boundary (some of them will encounter a reflection or two on the side boundaries). The intensity at the top boundary is known from the incoming solar radiation, thus the equation of transfer is solved recursively along the ray, until it reaches the point of origin. The boundary conditions at the ground surface can then be determined from Equation (7). The equation of transfer can then be solved along rays fired from the top boundary arriving at the ground.

3. DENSE GAS DISPERSION SIMULATION

The DT method was tested over simplified problems of geometry similar to typical dense gas dispersion situations. The aim of the testing procedure was mainly to validate the coding of the method and to provide confidence in its use in the dense gas dispersion model. For thorough tests of the DT method in one, two and three dimensions against analytical and experimental results, see Lockwood and Shah [9]. Here, a one-dimensional geometry of radiative transfer between two black infinite plates was tested. The DT method solution using 50 rays fired from

each wall is compared with the analytical solution of Heasalt and Warming [14] in Table I, which shows good agreement.

The resulting temperature distribution between the two walls that can be recovered from the energy sources in each element is shown in Figure 1, which also shows excellent agreement with the analytical solution of Heasalt and Warming. To test the sensitivity to the number of rays, several computations were performed with varying numbers of rays and the results are summarised in Table II.

The solution for the same geometry with one of the walls black and the other one grey, of emissivity of 0.8, was also obtained. The results are shown in Figure 2, where good agreement is observed.

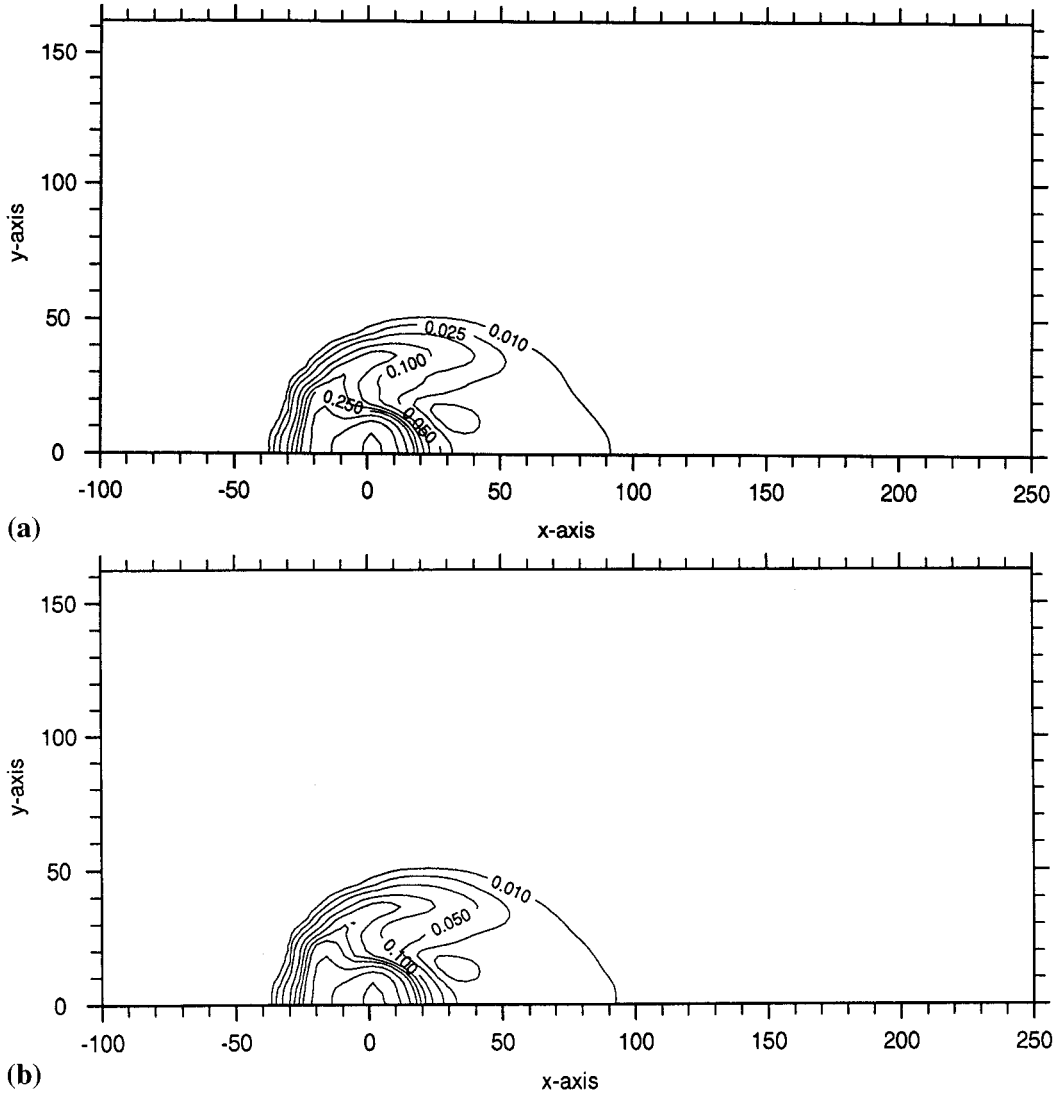

Figure 4. Dense gas contours at the horizontal plane $z = 0.76$ m after 32 s from the time the dense gas valve was fully opened, (a) no radiation modelling, (b) radiation effects modelled.

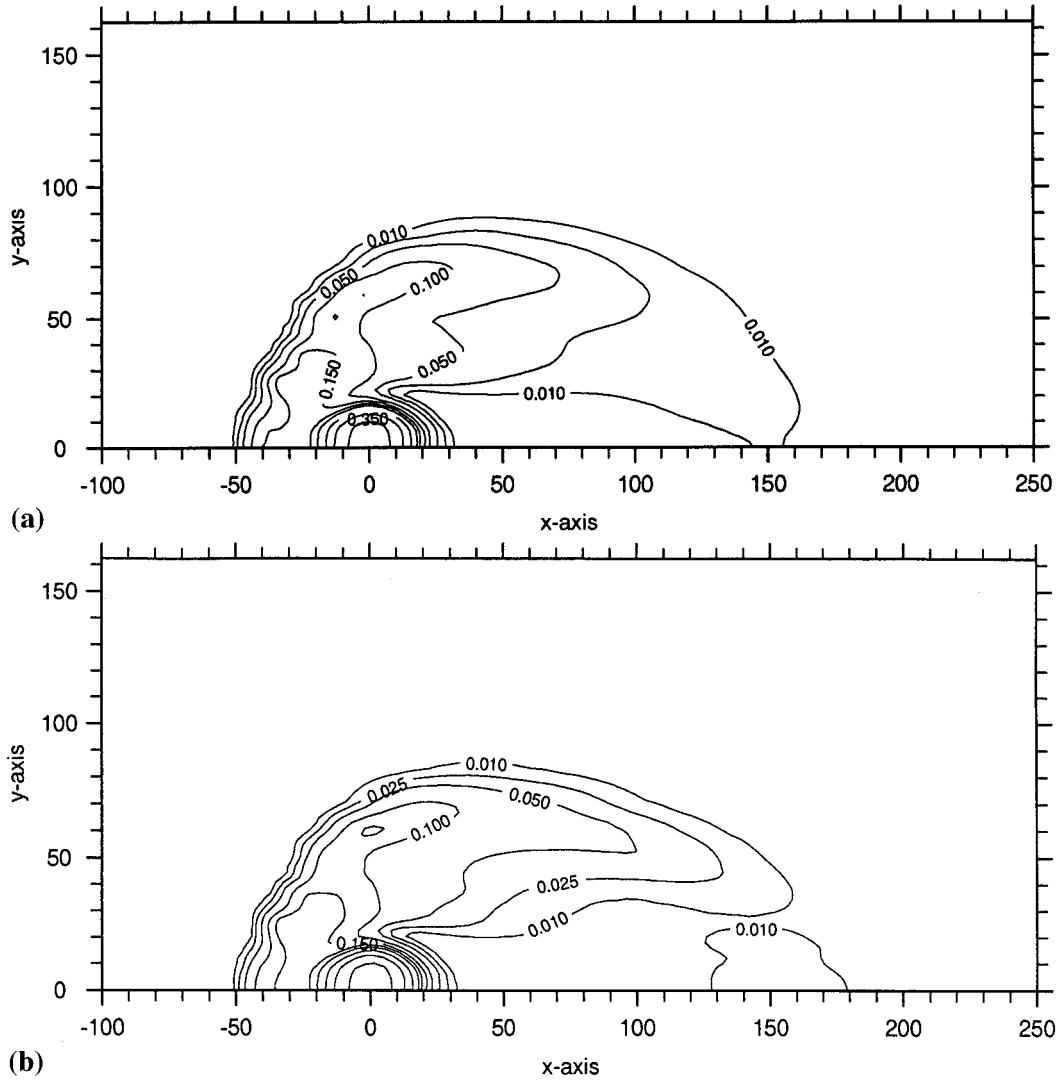

Figure 5. Dense gas contours at the horizontal plane $z = 0.76$ m after 76 s from the time the dense gas valve was fully opened, (a) no radiation modelling, (b) radiation effects modelled.

The Burro-8 test was modelled over flat ground to test the effects of the radiation model. This field test was conducted over gently undulating terrain and was approximated in this paper over flat grounds. This allows for half of the domain to be used in the solution, due to the symmetry along the central plane, without any loss of generality in verifying the performance of the radiation model. A schematic diagram of the solution domain in shown in Figure 3, where the source area of the dense gas is indicated. A rectangular finite element mesh was used of 30, 20 and 14 elements in the x-, y- and z-directions, respectively. Consequently, the mesh contained 8400 elements and 9765 nodal points. A simulation had been conducted successfully without the radiation model, and the results were presented in Reference [4] (also see Reference [7] for detailed results). These results showed that the model could predict the major features of the dense gas dispersion scenario. However, the simulation showed a lower and wider cloud than that obtained in the experiment.

Methane absorbs infrared radiation at four narrow bands. The absorption in the first two bands is very small, so a two-band model simulation was used with bands around v_3 of frequency 3020 cm^{-1} and v_4 of frequency 1306 cm^{-1}. The average absorption coefficients at these two bands were calculated from the experimental results of Kim [15]. This resulted in an absorption coefficient of 74.5 cm^{-1} for the absorbing interval of 400 cm^{-1} around v_3 and an average absorption coefficient of 73.0 cm^{-1} around the absorbing frequency interval of 200 cm^{-1} around v_4. The incoming solar radiation in the two bands was calculated, assuming that the sun is a black-body radiator of temperature 5800 K. No account was made for the reduction in the solar radiation due to absorption and scattering in the upper atmospheric

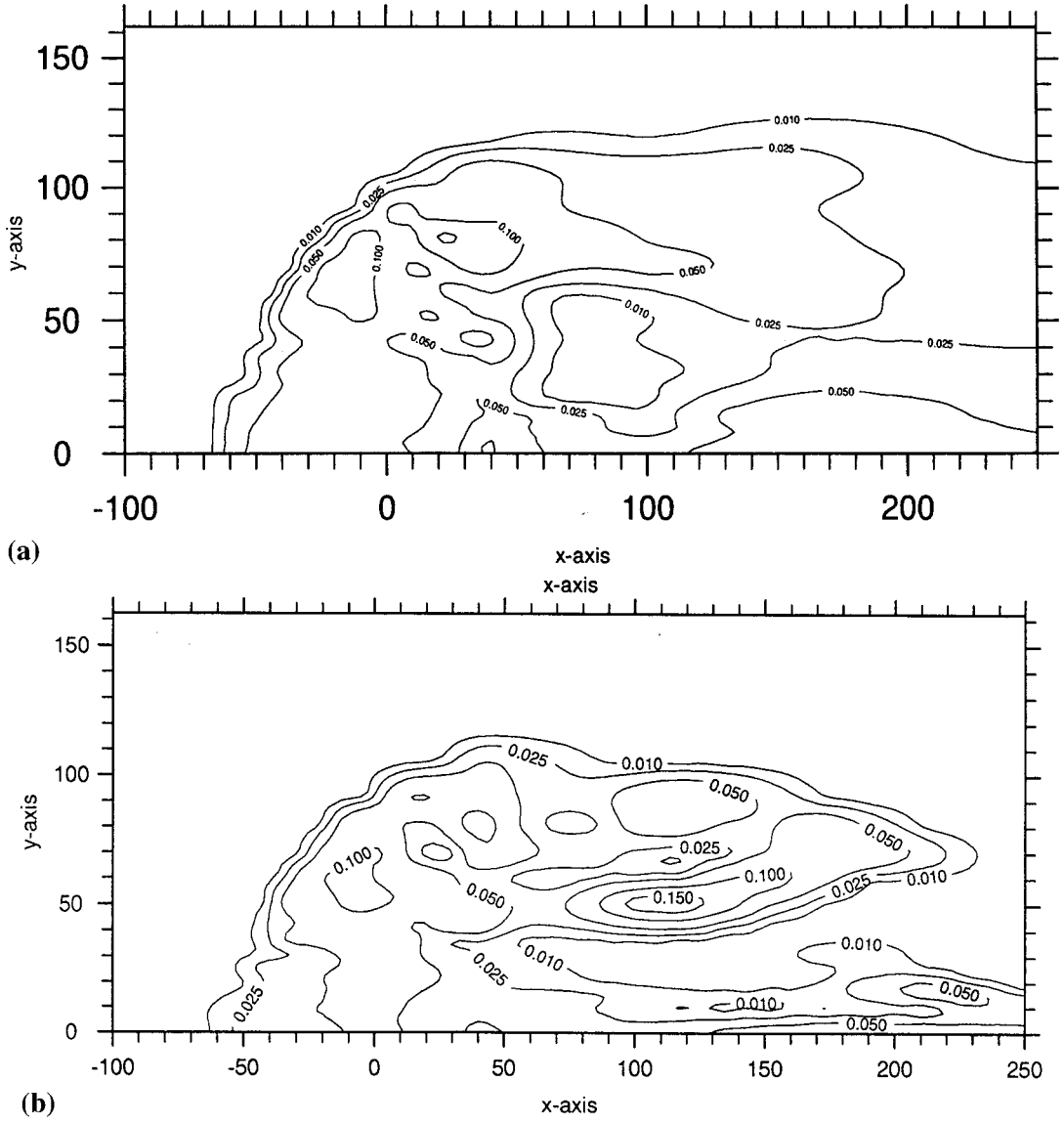

Figure 6. Dense gas contours at the horizontal plane $z = 0.76$ m after 174 s from the time the dense gas valve was fully opened, (a) no radiation modelling, (b) radiation effects modelled.

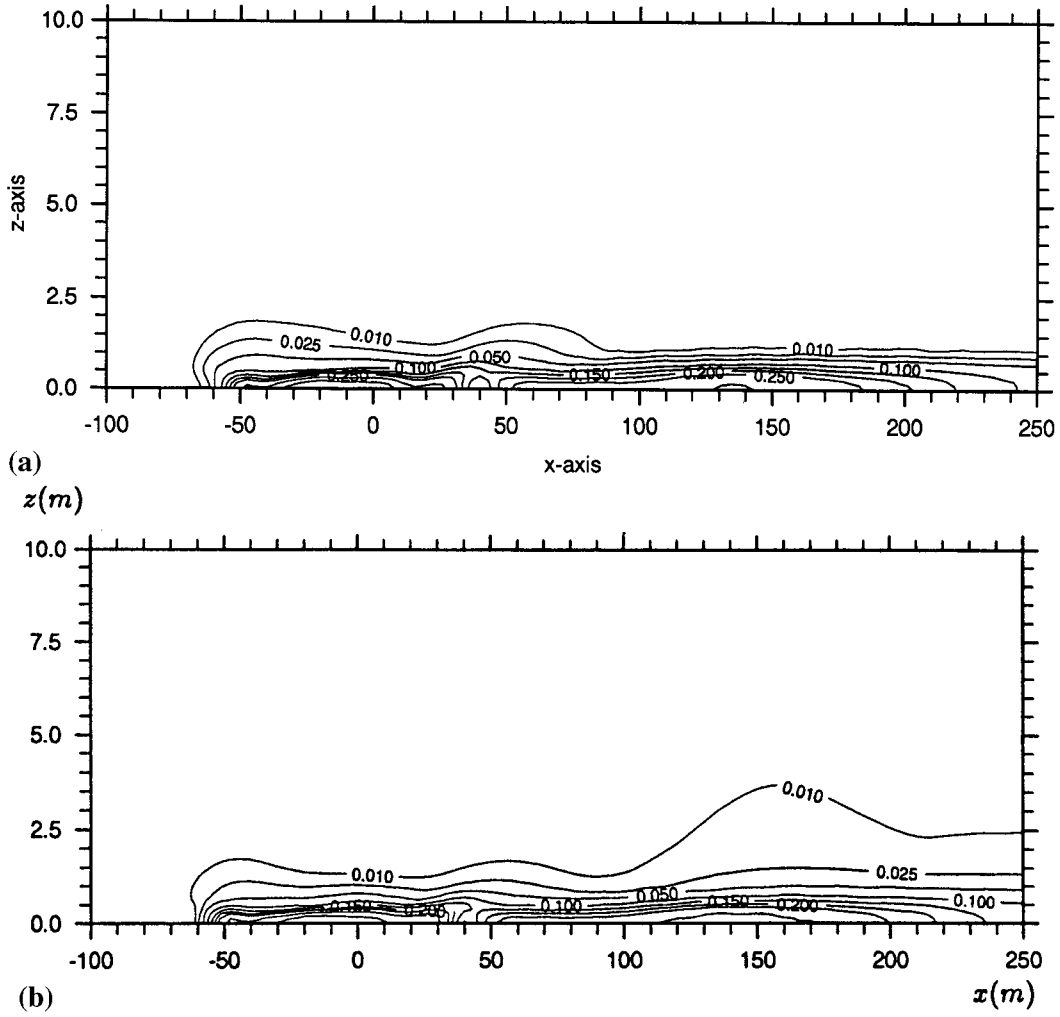

Figure 7. Dense gas contours at the vertical middle plane after 174 s from the time the dense gas valve was fully opened, (a) no radiation modelling, (b)radiation effects modelled.

layers since this will involve large uncertainties depending on different factors like atmospheric conditions and pollution levels. Furthermore, it was assumed that the incoming solar radiation is diffuse, i.e. it is not coming from one direction.

The two-band model used 20 rays, fired from each of the 1200 elements with surfaces at the ground and at the top boundary of the domain. The rays were distributed over four equal polar angles and five equal azimuth angles, to bring the total number of rays used to 24 000. These rays were traced geometrically in a preprocessor program and the information was stored for use in the flow solver to calculate the radiation sources in the energy equation at each time step. The inclusion of the radiation model led to a 20% increase in the total dense gas dispersion simulation time on the CRAY YMP-EL.

Figures 4–6 show horizontal concentration contours of the dense gas at times 32, 76 and 174 s, respectively, from the time the dense gas tap was fully opened, for the test cases with and

without the radiation model. Figure 7 shows the vertical concentration contours at the symmetry plane for the time 174 s for both simulations. At the initial stages of the simulation, the effects of the radiation absorption was not noticeable. Later, when the cloud grew in size, it was observed that the radiation effects led to a minor increase in the cloud height. However, this led to faster travel of the cloud in the wind direction and a narrower cloud, which improved the agreement with experimental results. Figure 8 summarises the results by showing the maximum distance travelled by the 5% volume concentration contour (lower flammability limit) at 1 m above ground level, compared with both the experimental results [5] and another simulation using FEMSET over the real irregular topography but without consideration of the radiation effects. This shows that the consideration of radiation absorption led to significant improvements in the predictions. Inclusion of radiation absorption effects in the irregular topography simulation is expected to produce the best match with the experiment.

A hypothetical test has also been conducted with a gas having absorption bands ten times larger than methane. The aim was to study the sensitivity of radiation effects and to provide an idea of the effects if other gases of wider or more absorption bands were involved. The simulation showed that radiation effects led to the dense gas cloud being transformed into a buoyant plume, 76 s after the start of the release. This can be seen from the contours of Figure 9.

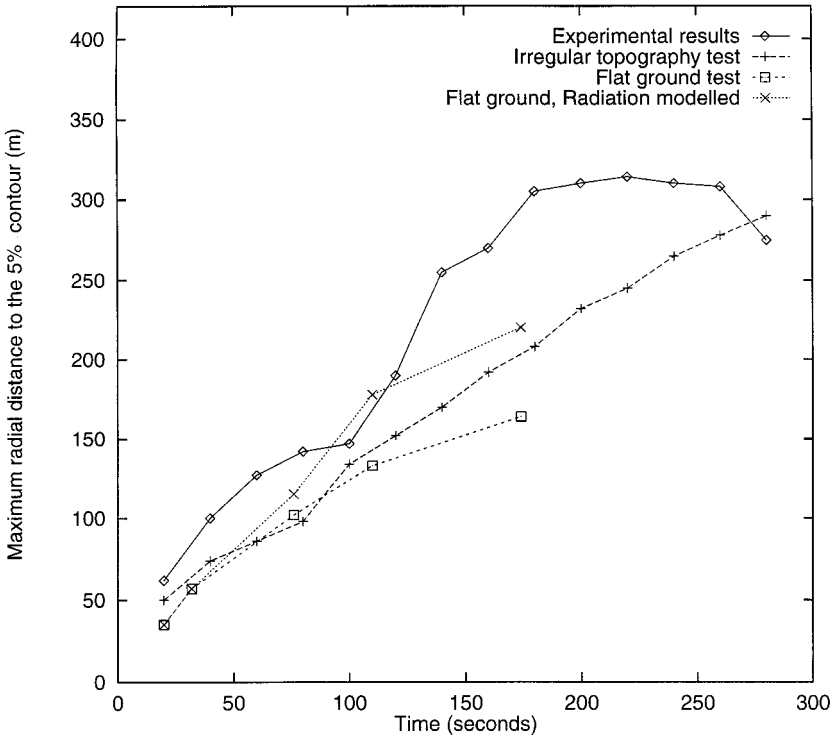

Figure 8. Maximum radial distance travelled by the lower flammability limit contour.

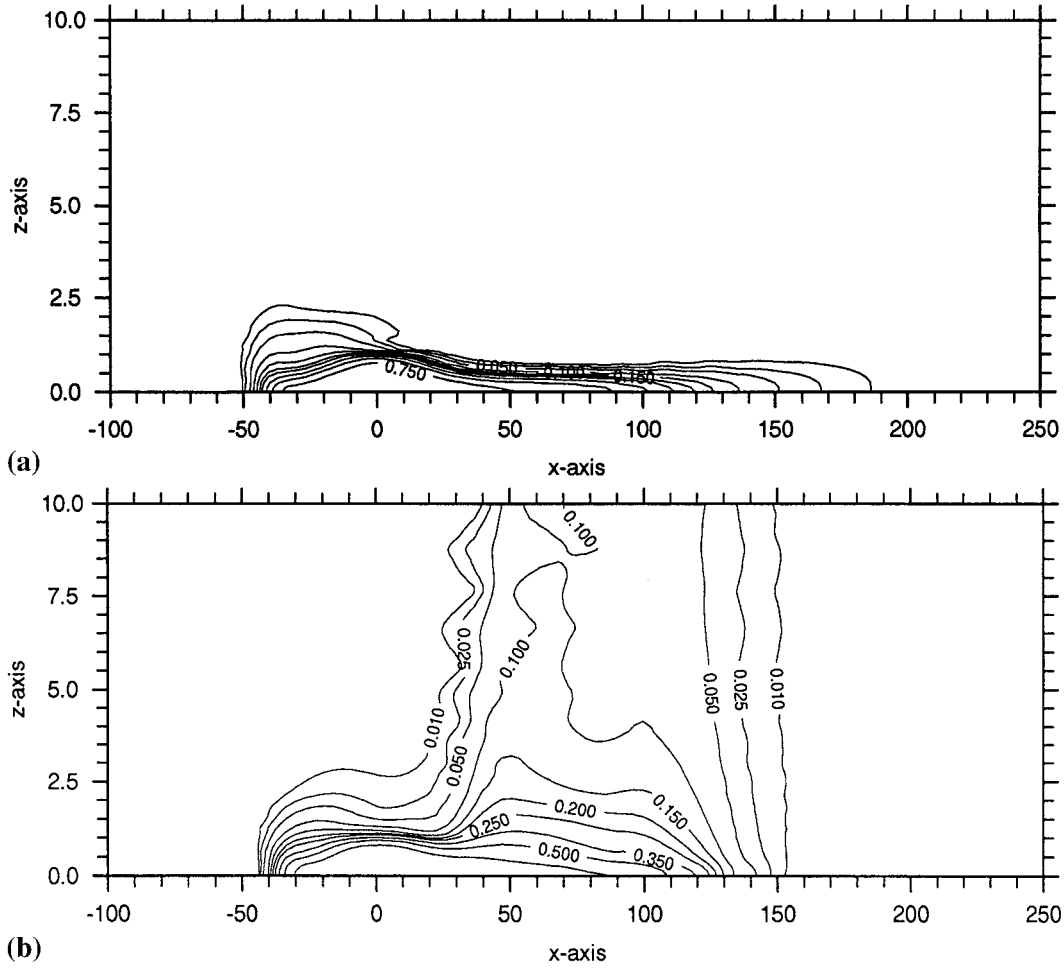

Figure 9. Concentration contours at the vertical middle plane after 76 s from starting the spill; (a) no radiation modelling, (b) radiation is modelled assuming a hypothetical gas.

4. CONCLUSIONS

It has been shown that the DT method is an efficient way to calculate radiation absorption effects on the dense gas dispersion process. Radiation absorption can be a significant factor in the total thermal balance of the process and should be taken into account. In the dispersion of gases of wide absorption bands or when large fires are present, radiation absorption may be dominant.

APPENDIX A. NOMENCLATURE

$B_v(T)$	Planck function for monochromatic emissive power
c	speed of light

$\underline{\mathrm{d}A}$	a vector of magnitude equal to a finite area and direction normal to the area
h	Planck's constant
I_v	monochromatic intensity of a beam of radiation
I_b	average intensity of a beam of radiation
I_0	average intensity of a beam of radiation at its origin
k	turbulent kinetic energy
k_v	monochromatic absorption coefficient
k_b	average absorption coefficient
S_e	heat source in an element due to radiation absorption
s	the path of a radiation beam
T	absolute temperature
T_w	wall temperature
t	time
$\hat{\Omega}$	the direction of a radiation beam
$\underline{\Omega}$	a unit vector in the direction of a beam
v	frequency of radiation
κ	Boltzman constant
σ	Stefan–Boltzman constant
ϵ	turbulent kinetic energy dissipation
ϵ_h	emissivity

REFERENCES

1. P.L. Betts and V. Haroutunian, 'Finite element calculations of transient dense gas dispersion', in J.S. Puttock (ed), *Stably Stratified Flow and Dense Gas Dispersion*, Clarendon Press, Oxford, 1988, pp. 349–384.
2. W. Rodi, *Tulrbulence Models and Their Applications—A State of the Art Review*, Int. Assoc. Hydraulics Research, Delft, Netherlands, 1980.
3. P.M. Gresho, S.T. Chan, R.L. Lee and C.D. Upson, 'A modified finite element method for solving the time-dependent incompressible Navier–Stokes equations: part 1', *Int. j. numer. methods fluids*, **4**, 557 (1984).
4. P.L. Betts and A.I. Sayma, 'Improved near ground treatment in finite element simulation of dense gas dispersion', in K. Morgan *et al.* (eds), *Finite Elements in Fluids*, Pineridge Press, Swansea, 1993, pp. 959–969.
5. A.I. Sayma and P.L. Betts, 'A finite element model for the simulation of dense gas dispersion in the atmosphere', *Int. j. numer. methods fluids*, **24**, 291–317 (1997).
6. P.L. Betts and M.M. El-Awad, 'Stability effects on dense gas dispersion: validation of turbulence model', in C. Taylor, J.H. Chin and G.M. Homsy (eds), *Proc. 7th Int. Conf. on Laminar and Turbulent Flows*, Stanford, 1991, Pineridge Press, Swansea, 1991, pp. 212–221.
7. A.I. Sayma, 'A finite element model for dense gas dispersion: effects of ground topography and radiation absorption', *Ph.D. Thesis*, Faculty of Technology, University of Manchester, 1994.
8. R.P. Koopman, J. Baker, R.T. Cederwall, H.C. Goldwire, W.J. Hogan, L.M. Kamppinen, R.D. Kiefer, J.W. McClure, T.G. McRae, D.L. Morgan, L.K. Morris, M.W. Spann and C.D. Lind, 'Burro series data report LLNL/NWC 1980 LNG spill tests', *Tech. Rep. UCID-19075*, Lawrence Livermore National Laboratory, 1982.
9. F.C. Lockwood and N.G. Shah, 'A new radiation solution method for incorporation in general combustion prediction procedures', *18th Symp. (Int.) on Combubstion*, The Combustion Institute, Pittsburgh, 1981, pp. 1405–1413.
10. S. Chandrasekhar, *Radiative Transfer*, Dover, New York, 1960.
11. H.C. Hotel and A.F. Sarofim, *Radiative Transfer*, McGraw-Hill, New York, 1967.
12. R. Siegel and J.R. Howell, *Thermal Radiation Heat Transfer*, McGraw-Hill, New York, 1972.
13. N.G. Shah, 'The computation of radiation heat transfer', *Ph.D. Thesis*, Imperial College of Science and Technology, 1979.
14. M.A. Heasalt and R.F. Warming, 'Radiative transport and wall temperature slip in an absorbing planar medium', *Int. J. Heat Mass Trans*o, **8**, 979–994 (1965).
15. K. Kim, 'Integrated infrared intensities of methane', *J. Quant. Spectrosc. Radiat. Trans.*, **37**, 107–110 (1987).

